

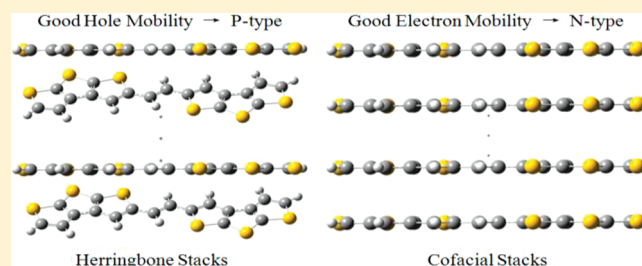
Electronic Structures and Charge Transport of Stacked Annulated β -Trithiophenes

Hongguang Liu, Sunwoo Kang, and Jin Yong Lee*

Department of Chemistry, Sungkyunkwan University, Suwon 440-746, Korea

ABSTRACT: Density functional theory (DFT) calculations were performed using a MPWB1K functional to interpret the charge transport (CT) properties of stacked annulated β -trithiophene molecules. The goal was to help understand how the chemical composition, face-to-face stacking, intra- and intermolecular correlations, and the applied electric field affect the CT properties of this organic semiconductor compared with those of the edge-to-face “herringbone” motif. The variations in the frontier molecular orbitals, energy gap, nonadiabatic electron attachment energies (EAE), and vertical detachment energies (VDE) were investigated under an external electric field as a function of the number of stacked layers (n).

Two possible CT pathways, monomer-to-monomer (MM) and dimer-to-dimer (DD) transports, were postulated to determine the charge carrier conductivities of these molecules. The results highlight that the intermolecular electronic couplings and electrostatic interactions can significantly affect the stacking geometry, even in more extended structures; displaced stacks with smaller interlayer spacing resulted in more compact stacking and, thus, higher CT efficiency; face-to-face stacking geometries can help to reduce the energy gap and VDE. Despite the fact that common thiophene-based oligomers adopting edge-to-face herringbone motifs exhibited p-type (hole-transporting) characters, the face-to-face stacked models based on annulated β -trithiophenes exhibited remarkably increased n-type (electron-transporting) performances. The electric field in the z -direction produced a small influence on the DD charge transport, whereas both electron and hole mobilities decreased dramatically in the MM case. More importantly, in MM charge transport, the electric field increases the hole mobility so that it is higher than that of the electron.



INTRODUCTION

Packed organic semiconductors are of current interest to many scientists due to their effective charge transport behavior, which can be widely utilized in various electronic devices, including solar cells, organic diodes, and field-effect transistors (OFETs).^{1–3} Among the most versatile organic semiconductors, thiophene-based oligomers are widely studied for use as p-type (hole-transporting) OFETs due to their good electron-donating properties and low electron affinities.⁴ Despite great progress in the exploration of high-performance p-type OFETs, a demanding objective for the continued advancement in the field of organic electronics is the development of conjugated oligomers that enable the invention of n-type (electron-transporting) OFETs.⁵ However, excellent n-type organic semiconductors with ideal packing arrangement, high electron affinities, high electron mobility, and good environmental stability are still scarce.^{5a,6} To realize high-performance n-type OFETs, these materials should have (i) an optimal packing orientation that results in increased orbital overlap, (ii) a lower LUMO energy level that facilitates electron injection, and (iii) ideal environmental stability. Recently, it has been systematically determined that some oligothiophenes incorporated with electron-withdrawing groups lower the LUMO energy levels and produce n-type OFETs.⁷ Although these materials have suitable LUMO energies, many of them lack sufficient intermolecular interactions,⁸ which may restrict the electron transport

and thus decrease the performance of n-type OFETs. Little attention has been paid to the electron conductivity change in certain oligothiophenes induced by variation in the packing motif; for example, from herringbone to cofacial stacking.

Several XRD studies of some popular OFETs, including oligoacenes and pentacene, which adopt a herringbone formation in which the molecules are packed edge-to-face between layers, have shown that these formations result in the highest carrier mobilities.^{9–11} However, the herringbone packing arrangement somehow limits the realization of their potentially high carrier mobility^{12,13} due to the fact that the edge-to-face motif minimizes the effective π – π overlap between adjacent molecules. From the viewpoint of bandwidth and the hopping theory of carrier conduction, face-to-face a stacking motif is highly desirable for achieving higher mobility.¹⁴ Experimental evidence that a π -stacking geometry results in better mobility in the solid state than does the herringbone motif is still limited. However, overcoming the difficulties of single crystal growth and device fabrication will allow for the preparation of additional π -stacking materials.¹⁵

Special Issue: Shaul Mukamel Festschrift

Received: May 19, 2010

Revised: October 16, 2010

Published: November 03, 2010

Recently, Aso et al.^{7b,c} and Yamashita et al.¹⁶ have reported that several S-containing heterocyclic oligomers exhibited a low LUMO level, a densely packing structure, and a good n-type OFET performance. The heterocyclic units, such as thiophene⁷ and thiazole,¹⁶ can improve the intermolecular interactions due to π - π stacking as well as heteroatom contact. Difluoromethylene-bridged oligothiophenes synthesized by Yoshio et al. displayed a favorable face-to-face π -stacking pattern with regular intervals (3.6 Å). Devices based on these materials show n-type OFET behavior with an electron mobility of $1.8 \times 10^{-2} \text{ cm}^2 \text{ V}^{-1} \text{ s}^{-1}$.⁵ These findings should encourage the unveiling of more S-containing oligomers for n-type OFET.

Consisting of fused trithiophene units, a novel type of organic semiconductor based on annelated β -trithiophenes, *trans*-1,2-(dithieno[2,3-*b*:3',2'-*d'*]-thiophene)ethane, was successfully synthesized by Tan et al.¹⁷ It was reported that the device incorporating this compound adopted a compressed herringbone motif and exhibited a p-type character with a maximum hole mobility of $0.89 \text{ cm}^2 \text{ V}^{-1} \text{ s}^{-1}$. Although theoretical simulations were performed to analyze the hole transport efficiency based on the experimental results, no attention was given to the electron transport, which was also facilitated by increased π - π interactions. The enhancement in electron transport efficiency is commonly overlooked, since the material should be p-type.¹⁸

The fused-ring thiophene derivatives are of interest because (i) molecules having fused ring systems tend to maximize π -orbital overlap by restricting intramolecular rotation in the oligomer, possibly inducing highly ordered π -stacking,¹⁹ and (ii) S-containing heterocyclic oligomers display many advantages over other candidates with regard to the production of n-type OFET.¹⁶ By changing the stacking motif from herringbone to cofacial, the electron mobility can be dramatically increased and may even surpass the hole mobility.

Two mechanisms are generally discussed when considering charge transport: superexchange and hopping (sequential). Charge transfer through molecular bridge between a donor and an acceptor is generally recognized as a superexchange mechanism in which the charge tunneling occurs without the transient occupation of the bridge states.^{20,21} In the hopping mechanism, the bridge is more directly involved in the CT process,²² and the charge temporarily resides in the intermediate state. In superexchange, the only role of this intermediate state is that of a virtual state.²³ The hopping mechanism is less efficient for short bridges than is the superexchange pathway, whereas the latter pathway may be overwhelmed by intrabridge hopping in the case of long bridges.²⁴ In the superexchange process, long-range CT increases through the indirect mixing of the orbitals of the donor and acceptor wave functions.²³ It has been noted that cofacial π - π stacking can render more effective orbital overlap and thus higher electronic coupling that promotes carrier hopping between molecules.^{14,25} At room temperature, the OFET charge is believed to be localized in individual molecules, and the CT mechanism is a hopping mechanism that can be described by the Marcus theory.²⁶

Here, we studied the electronic structures and charge carrier mobilities for one-dimensional cofacial stacking of annelated β -trithiophenes molecules. To understand the charge transport properties of this organic semiconductor, several factors, including chemical composition, stacking geometry, intra- and intermolecular correlations, and applied electric field, are considered.

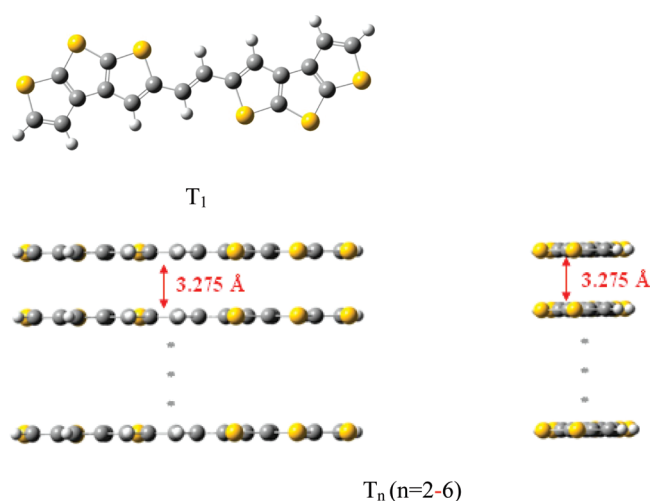


Figure 1. Initial structures of the annelated β -trithiophenes, T_1 , and its stacked conformers, T_n ($n = 2-6$).

COMPUTATIONAL METHODS

The second-order Møller–Plesset perturbation theory (MP2) is commonly used to describe electron correlations for intermolecular π - π interaction systems. However, the MP2 method is time-consuming and can rarely be applied to large molecular structures. In contrast to MP2 method, the density functional theory (DFT) has been successfully employed to large molecules and large-scale systems due to its fast computational speed. In addition to the salient efficiency of the theory, DFT has been found to be reasonably accurate for calculating the chemical and structural properties of species, such as organic semiconductors and conventional inorganic semiconductors.^{27–36} Among the tested hybrid meta DFT protocols, MPWB1K provides the best results for the combination of thermochemistry, thermochemical kinetics, hydrogen bonding, and weak interactions.³⁷ The MPWB1K functional has also been shown to be adequate for the study of π -stacking, H-bonding interactions^{38a} and CH/ π interactions.^{38b} Therefore, as a useful DFT method that provides the best performance in charge-transfer interactions,^{37b} MPWB1K is ideal for analyzing the CT properties in our stacked models.

The initial stacked models (T_2 , T_3 , T_4 , T_5 , and T_6) had well-designed conformations, adopting cofacial juxtapositions with an identical intermolecular distance of 3.275 Å, as shown in Figure 1. This initial value was selected due to the fact that the close S...S contacts (as short as 3.34 Å) were obtained through single-crystal X-ray diffraction (XRD) structure analysis.¹⁷ This extremely short contact (3.34 Å) was one of the shortest S...S distances reported in sulfur-decorated organic semiconductors.³⁹ It is widely accepted that cofacial molecular arrangement within twice the van der Waals radius of an S atom (4.0 Å) is responsible for more effective CT due to uniform intermolecular orbital overlap. To investigate the CT nature, a single layer of annelated β -trithiophenes (T_1) and its stacked conformers (T_2 , T_3 , T_4 , T_5 , and T_6) were performed with DFT using MPWB1K in association with the 3-21G* basis sets, employing a suite of Gaussian 03 programs.⁴⁰ The variations in molecular structure and their corresponding CT properties under an applied electric field were also investigated. For the electric field condition, a finite electric dipole field of 0.05 V/Å was separately applied along each Cartesian axis. Nonadiabatic electron attachment energies (EAE) and vertical detachment energies (VDE) were also

considered. The EAE/VDE were defined as $E(T_n^-)/E(T_n^+) - E(T_n)$, where $E(T_n^-)/E(T_n^+)$ and $E(T_n)$ denote the energies of anions/cations at the neutral optimized geometries and the neutral energy, respectively.

At room temperature, the charge transport in the OFET can be well described as a hopping mechanism. The CT rate between two neighboring molecules can be calculated using the Marcus theory:²⁶

$$k_{CT} = \frac{4\pi^2}{h} \frac{1}{\sqrt{4\pi\lambda k_B T}} t^2 \exp\left(-\frac{\lambda}{4k_B T}\right) \quad (1)$$

There are two major parameters that determine the self-exchange CT rate: the transfer integral (t) and the internal reorganization energy (λ). In this context, the absolute value of transfer integral t for electron and hole transports is approximated using the Koopmans' theorem (KT),⁴¹ relying on the one-electron approximation. The absolute value of the transfer integral for electron [hole] transfer is approximated as

$$t = \frac{E_{L+1[H]} - E_{L[H-1]}}{2} \quad (2)$$

where $E_{L[H]}$ and $E_{L+1[H-1]}$ are the energies of the LUMO and LUMO+1 [HOMO and HOMO-1] in the closed-shell configuration of the neutral state, respectively.

Optimized dimer (T_2) and tetramer (T_4) geometries are used to approximate monomer-to-monomer transport and dimer-to-dimer transport, respectively. The total internal reorganization energy, λ , can be obtained as the sum of two relaxation energy terms: (i) the difference between the energies of the neutral molecule in its equilibrium geometry and in the relaxed geometry characteristic of the radical ion and (ii) the difference between the energies of the radical ion in its equilibrium geometry and in the neutral geometry. The diffusion coefficient, D , of charge carriers can be calculated using the Einstein–Smoluchowski equation (eq 3),⁴² where L is the effective length of the CT (approximated by the molecular center-to-center distance of a dimer). The charge carrier mobilities are evaluated using the Einstein relation (eq 4),⁴² where e is the electronic charge, k_B is the Boltzmann constant, and T is the temperature in Kelvin (298 K in this study). This method and its variations have been employed for the theoretical predictions of the charge carrier mobilities of organic semiconductors.⁴³

$$D = L^2 k_{CT} / 2 \quad (3)$$

$$\mu = eD / k_B T \quad (4)$$

RESULTS AND DISCUSSION

Among the calculated structures with no applied electric field, monomer T_1 nearly maintained its planar conformation, whereas T_2 underwent a slight geometric change with an increased distance between the two segregated stacks (close $S \cdots S$ contacts increased to 3.6 Å, on average, nearly equivalent to that of the difluoromethylene-bridged oligothiophenes synthesized by Yoshio et al., indicating that the cofacial stacked thiophene-based oligomers may have similar intervals between layers). Moreover, in each single layer of T_2 , a torsional angle of 5.2° was observed between two trithiophene units, which might attribute to the existence of those strong $S \cdots S$ electronic couplings⁴⁴ and the unfavorable π -electron repulsions.⁴⁵ Similar distortions also exist

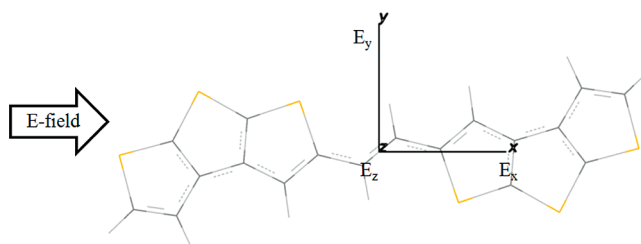


Figure 2. T_n ($n = 1-6$) with respect to an applied electric field along each Cartesian axis: E_x , E_y , E_z (For convenience, E_x , E_y , and E_z are defined as the electric fields applied along the x , y , and z axes, respectively; the z -axis is perpendicular to the molecular plane and exits the paper toward the reader).

in T_3-T_6 , indicating that these torsional angles derived from the intermolecular couplings and electrostatic repulsions can affect the entire stacking orientation, even in more extended structures. Through torsional rotation, the conjugation length can be effectively shortened,⁴⁶ which may reduce the CT along the intramolecular direction. As the number of layers (n) increased from 2 to 6, the largest torsional angle increased, 5.2° for T_2 and 14° for T_6 . In comparison with those of the dimer, the torsional angles in each stack of T_3-T_6 varied slightly from one another. It was interesting to observe that in T_3-T_6 , the middle layers had the smallest torsional angles, and this trend was maintained even when the electric field was applied. In addition, in these layers, the cofacial stacking geometry was converted to that of displaced stacks with smaller spacings, as the molecules were never exactly stacked due to a perfect cofacial situation in which the electrostatic repulsion terms were at their maximum.¹⁸ As a result, displacement often occurred along the molecular axes between neighboring molecules. Compared with T_2 , the spacings between adjacent molecules were greatly condensed (the closest intermolecular distance was shorter than 3.275 Å). However, the close $S \cdots S$ contacts maintained approximately the same distance, 3.6 Å, in the dimer formation, indicating that the strong $S \cdots S$ interactions and electrostatic interactions still significantly affect the stacking geometry in the more extended structures. Since CT was assumed to occur via the hopping mechanism, if the orbital overlaps were not greatly decreased, then the CT rate was increased due to the reduced intermolecular distance.¹³

To garner more insight into the molecular electronic structures, the highest occupied molecular orbitals ($HOMO_n$) and the lowest unoccupied molecular orbitals ($LUMO_n$) of T_n ($n = 1-6$) were investigated and are shown in Figure 3. For $n = 1$ and 2, the HOMO electrons were completely delocalized over all of the layers; however, for $n = 3$, most HOMO electrons were localized over the central layer, with some electrons in the terminal layers. These special electron distributions may result from the minimal torsional angles observed in the middle layer. For $n > 3$, the HOMO electrons were distributed over the three central layers in patterns similar to that in T_3 , as shown in Figure 3. The LUMO shapes indicated a diffused electron distribution, and delocalization of the LUMO over the whole conjugated system suppressed the charge recombination, allowing for long-lived anion species and facilitating electron movement. Thus, this strong interlayer orbital overlap in LUMO suggests that annelated β -trithiophenes should be good candidates for n -type molecular electronic device materials because the LUMO is believed to be important in the electron transport. A close examination revealed that the strong interlayer orbital overlap was due to the $\pi-\pi$ interactions of



Figure 3. Highest occupied molecular orbitals (HOMO_n) and lowest unoccupied molecular orbitals (LUMO_n) of T_n ($n = 1-6$) in the absence of an external electric field.

$\text{C} \cdots \text{C}$ and the p orbital interactions of $\text{S} \cdots \text{S}$ and $\text{C} \cdots \text{C}$. The overlap of electronic wave functions and thus the transfer integral depends on the intermolecular distance and orientation.¹⁴ On the basis of the LUMOs, the hopping process is possible for up to four and five layers because the LUMOs showed interlayer orbital overlap up to T_4 and T_5 , but the terminal T_6 LUMO layer was not involved in the orbital overlap. Therefore, for layered systems of annelated β -trithiophenes greater than T_6 , both hopping and superexchange mechanisms may be responsible for electron transport.

When an electric field is applied, the shapes of the molecular orbitals and molecular structures will change, subsequently modifying the conductivity through the molecule. Moreover, depending on the direction of the applied electric field (perpendicular or parallel to the molecular plane), the conductivity may produce a different response. To investigate such differences, an electric field was applied to T_1-T_6 along each Cartesian axis (Figure 2). The results show that the general stacking geometries (of T_2-T_6)

were not interrupted by exposure to an external electric field and that the strong $\text{S} \cdots \text{S}$ interactions still existed with close $\text{S} \cdots \text{S}$ contacts of ~ 3.6 Å. Compared with the condition in which no electric field was applied, the largest torsional angles increased when the fields were applied to the lower packing modes (T_1-T_3), whereas for higher packing modes (T_4-T_6), the torsional angles were smaller than those to which no electric field was applied (Figure 4). These variations indicate that for the stacked structure, an applied electric field along the three Cartesian axes may help to decrease the torsional angles, thus facilitating intramolecular CT.

The calculated HOMO and LUMO energies and energy gaps of T_n under the applied electric field in the x , y , and z directions are displayed in Figure 5. In the absence of an electric field, the HOMO and LUMO energies increased as the n increased, although the HOMO energy increased even further. Thus, the energy gap decreases as n increases. The increased HOMO energy level with increasing n facilitates the formation of radical

cations (holes) at the interface between a dielectric and the semiconducting layer.¹⁹ When no electric field is applied, the values of the HOMO level ranging from 5.33 to 6.07 eV were lower than those of most polythiophenes and pentacene,¹⁹ indicating a higher oxidative stability. It is also worth noting that HOMO-1 and HOMO-2 share a trend similar to HOMO, and they were quite close to HOMO with regard to energy when $n \geq 3$. Such phenomena were observed in LUMO, for which the specific orbitals contributed to facilitate the electron injection, thus inducing a higher electron mobility. Under the influence of the electric field in any of the three directions, the HOMO energy increased more than did the corresponding LUMO energy of the stacked models ($n > 2$) compared with those in the absence of an electric field. The electric field in the z direction provided a more profound effect than did those in the x and y directions, as shown in Figure 5. Thus, on the basis of the stacked molecules, E_z (the electric field in the stacking direction) had a greater impact on the electrical conductivity. Of all the calculated structures, T_2 showed

the lowest HOMO–LUMO gap (4.16 eV), attributed to the ideal cofacial geometry.^{18,25} In comparison with the energy gap of pentacene (approximately 1.85 eV from the absorption edge),⁴⁷ the energy gaps of our packing models were much higher, suggesting higher redox stabilities.

Figure 6 shows the orbital energy changes and the HOMO–LUMO gap of T_4 with a field strength of E_z . The increments of the occupied orbital energies were larger than those of the unoccupied orbital energies at an increasing field strength; hence, the HOMO–LUMO gap dramatically decreased. By tuning the field strength of E_z , the energy gaps of these stacked molecules can be easily controlled; however, whether this kind of electric field facilitates or blocks CT requires further investigation.

The nonadiabatic EAE and the VDE can be calculated by adding or removing an electron from the stacked systems. As shown in Figure 7a, E_z exhibits entirely different effects on EAE compared with those of E_x and E_y . EAE increases logarithmically with n , suggesting that multistacked annelated β -trithiophene molecules lose their ability to hold an electron under E_z . Therefore, electrons moving through the LUMO will be blocked. Considering this, for higher stacked systems, it is expected that the electric field in the z direction will efficiently reduce the electron conductivity through the molecules, and this result is further confirmed by an electron mobility calculation. Figure 7b indicates that the VDE values were nearly inversely proportional to the size; that is, proportional to $1/n$. Similar size effects on the ionization potentials were predictable due to the fact that common relationships between VDE and ionization potentials exist in stacked species.^{48,49} By applying an electric field, the nonadiabatic EAE and the VDE can be controlled.

Charge mobility calculations were performed to obtain more insight into the charge transport properties of these stacking molecules. Table 1 lists CT parameters based on theoretical calculations of the cofacial stacked dimer (T_2) and tetramer (T_4). The charge transport pathways were investigated by considering two types of transport processes; monomer-to-monomer (MM) transport in T_2 and dimer-to-dimer (DD) transport in T_4 . Because the reorganization energies of electrons ($\lambda^- = 0.28$ eV) and holes ($\lambda^+ = 0.29$ eV) are nearly the same in MM transport, the transfer

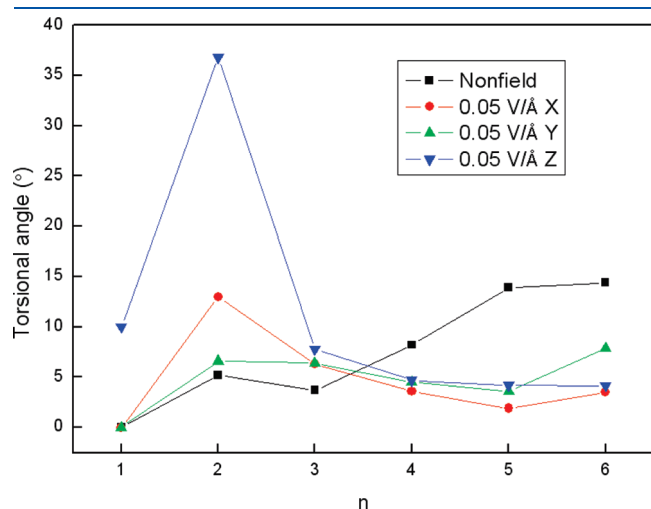


Figure 4. The largest torsional angles observed in each packing mode (T_1 – T_6) in the presence and absence of an electric field along each axis.

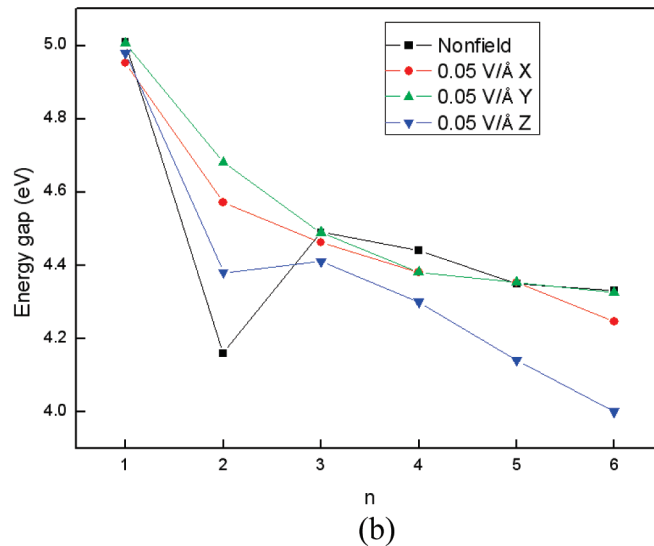
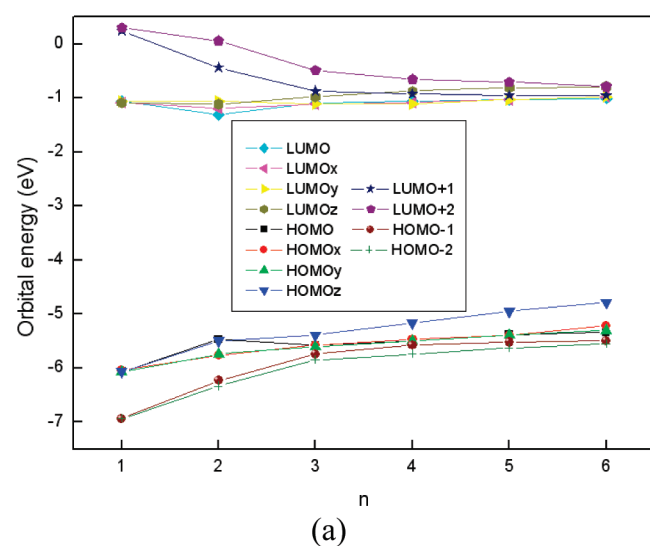


Figure 5. Changes in (a) frontier orbital energies and (b) energy gaps of T_n under the applied electric field of 0.05 V/Å in the x , y , and z directions. HOMO $_j$ and LUMO $_j$ denote the HOMO and LUMO energies when the field is applied along the j axis.

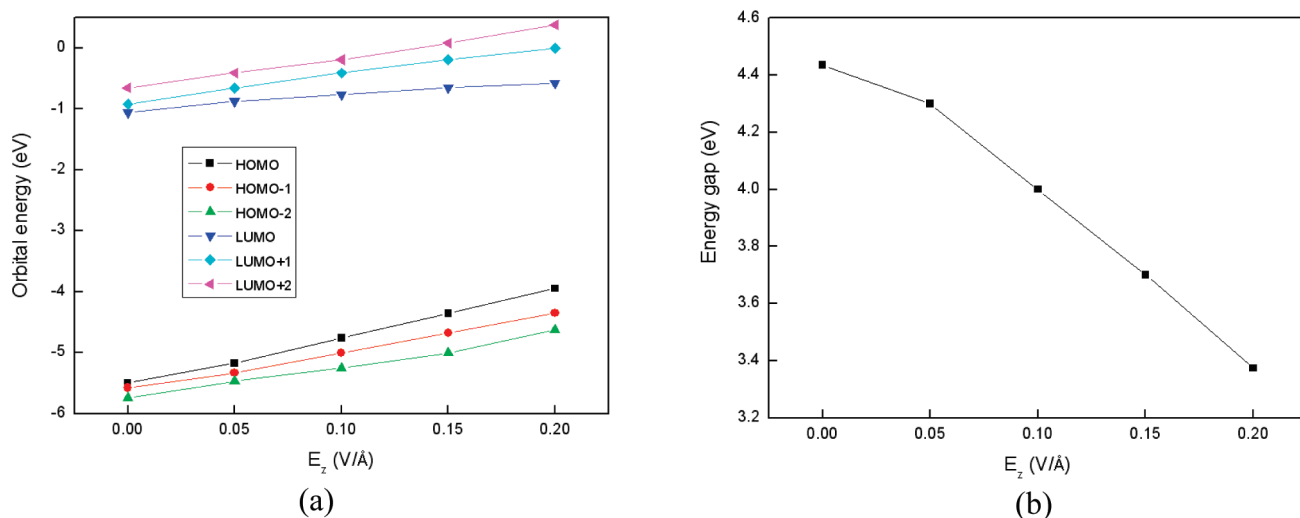


Figure 6. Changes in (a) frontier orbital energies and (b) the energy gap of T₄ as a function of the applied electric field strength in the z direction.

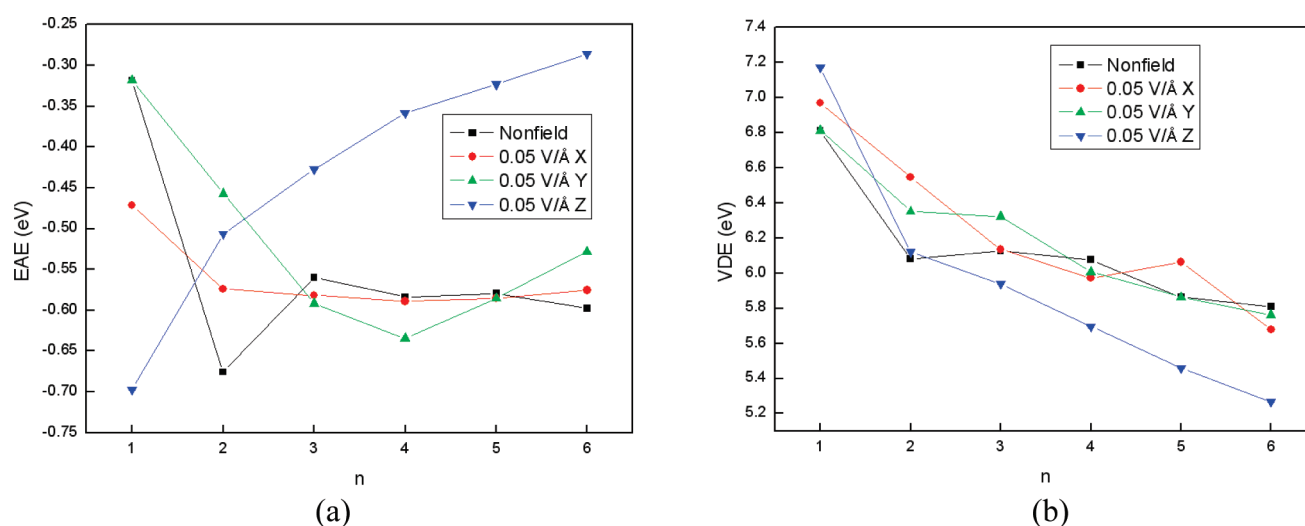


Figure 7. (a) Nonadiabatic electron attachment energies (EAE) and (b) nonadiabatic vertical detachment energies (VDE) with respect to an applied electric field.

Table 1. Charge Transport Parameters of a Stacking Dimer (T₂) and Tetramer (T₄) in the Presence or Absence of an Electric Field, Calculated at the MPWB1K/3-21G* Level

compound	t^+ (eV)	λ^+ (eV)	k^+ (s ⁻¹)	μ^+ [cm ² /(Vs)]	t^- (eV)	λ^- (eV)	k^- (s ⁻¹)	μ^- [cm ² /(Vs)]
T ₂	0.38	0.29	2.72×10^{14}	6.20	0.44	0.28	3.76×10^{14}	8.58
T ₂ ^a	0.37	0.37	1.04×10^{14}	2.36	0.27	0.38	5.22×10^{13}	1.19
T ₄	0.04	0.70	3.52×10^{10}	0.003	0.07	0.28	9.72×10^{12}	0.86
T ₄ ^a	0.08	0.64	2.88×10^{11}	0.03	0.11	0.30	1.94×10^{13}	1.73
experiment ^b				0.89				

^a Electric field is applied in the z direction. ^b Experimental data based on annelated β -trithiophenes arranged in a herringbone motif.¹⁷ +, Parameters of holes. -, Parameters of electrons.

rate and mobility depend mainly on the transfer integral. Because t^- in T₂ shows a larger value than t^+ , higher k^- and μ^- were induced; therefore, the electron transport was more efficient than the hole. When an electric field was applied in T₂, the energy difference (0.01 eV) between λ^+ and λ^- was still small, although the charge transfer rates and charge mobilities were obviously decreased due to increased reorganization energies. Most

interestingly, t^+ became larger than t^- , resulting in a reversed CT efficiency. That is, the hole transport was more dominant than was the electron transport. As we referred to DD transport in T₄, it is clear that both t^+ and t^- decreased, possibly due to the reduced effective orbital overlaps in T₄ compared with those in T₂. There was another distinct change in the reorganization energy for a hole in T₄, and λ^+ was more than twice that in T₂,

whereas λ^- hardly changed. On the basis of these considerations, the hole transport in the DD process was dramatically reduced. In addition, the electric field produced only minor effects in T_4 . The large reorganization energy of the hole significantly limited the hole conductivity during DD transport. Additional factors that were not considered in this study may have had an effect on the charge transport. For example, it is well-known that the charge transport depends heavily on the extent of order or disorder of the molecules in fabricated devices as well as on the temperature. Nevertheless, the molecular charge transport property provides good information for potential organic semiconductors, although the order control of the compounds has yet to be elucidated.

CONCLUSIONS

The electronic structures, frontier molecular orbitals, energy gaps, nonadiabatic electron attachment energies (EAE), vertical detachment energies (VDE), and charge mobilities were investigated on the basis of annelated β -trithiophenes via DFT calculations. The intermolecular electronic couplings and electrostatic interactions significantly affected the stacking geometry, even in more extended structures; displaced stacks with smaller interlayer spacing result in more compact stacking and, thus, higher CT efficiency; face-to-face stacking geometries may help to reduce the energy gap and VDE. In addition, decreased LUMO, LUMO+1, and LUMO+2 and increased HOMO, HOMO-1, and HOMO-2 energies for n may facilitate the electron injection, thus allowing for more efficient electron injection into the conjugated system and the induction of higher electron mobility. Although common thiophene-based oligomers adopting edge-to-face herringbone motifs show p-type (hole-transporting) characters, surprisingly, the face-to-face stacked models based on annelated β -trithiophenes exhibited remarkably increased n-type (electron-transporting) performances. The electric field in the z direction showed minor influences on DD charge transport, whereas for the MM case, both electron and hole mobilities were dramatically decreased. On the basis of these results, the electric field more greatly impacted the hole mobility than it did that of the electron. These results will be helpful in the design and control of devices incorporated with annelated β -trithiophene molecules to achieve better electron transport efficiency.

AUTHOR INFORMATION

Corresponding Author

* Phone: +82-31-299-4560. Fax: +82-31-290-7075. E-mail: jinylee@skku.edu.

ACKNOWLEDGMENT

This work was supported by the National Research Foundation (NRF) Grants 2010-0001630 and 2010-0000166 funded by MEST and by a grant from the Fundamental R&D Program for Core Technology of Materials funded by the Ministry of Knowledge and Economy, Republic of Korea.

REFERENCES

(1) Katz, H. E.; Lovinger, A. J.; Johnson, J.; Kloc, C.; Slegrist, T.; Li, W.; Lin, Y. Y.; Dodabalapur, A. *Nature* **2000**, *404*, 478.
(2) Yu, G.; Gao, J.; Hummelen, J. C.; Wudl, F.; Heeger, A. J. *Science* **1995**, *270*, 1789.

(3) Sirringhaus, H.; Tessler, N.; Friend, R. H. *Science* **1998**, *280*, 1741.
(4) (a) Katz, H. E.; Bao, Z. N.; Gilat, S. L. *Acc. Chem. Res.* **2001**, *34*, 359.
(b) Otsubo, T.; Aso, Y.; Takimiya, K. *J. Mater. Chem.* **2002**, *12*, 2565.
(5) (a) Newman, C. R.; Frisbie, C. D.; da Silva, D. A.; Brédas, J. L.; Ewbank, P. C.; Mann, K. R. *Chem. Mater.* **2004**, *16*, 4436. (b) Facchetti, A.; Yoon, M. H.; Marks, T. J. *Adv. Mater.* **2005**, *17*, 1705.
(6) Zaumseil, J.; Sirringhaus, H. *Chem. Rev.* **2007**, *107*, 1296.
(7) (a) Cai, X. Y.; Burand, M. W.; Newman, C. R.; da Silva, D. A.; Pappenfus, T. M.; Bader, M. M.; Brédas, J. L.; Mann, K. R.; Frisbie, C. D. *J. Phys. Chem. B* **2006**, *110*, 14590. (b) Ie, Y.; Nitani, M.; Ishikawa, M.; Nakayama, K.; Tada, H.; Kaneda, T.; Aso, Y. *Org. Lett.* **2007**, *9*, 2115. (c) Ie, Y.; Umemoto, Y.; Okabe, M.; Kusunoki, T.; Nakayama, K. I.; Pu, Y. J.; Kido, J.; Tada, H.; Aso, Y. *Org. Lett.* **2008**, *10*, 833.
(8) (a) Sakamoto, Y.; Suzuki, T.; Kobayashi, M.; Gao, Y.; Fukai, Y.; Inoue, Y.; Sato, F.; Tokito, S. *J. Am. Chem. Soc.* **2004**, *126*, 8138. (b) Cornil, J.; Beljonne, D.; Calbert, J. P.; Brédas, J. L. *Adv. Mater.* **2001**, *13*, 1053.
(9) Lin, Y. Y.; Gundlach, D. J.; Jackson, T. N. *Annu. Device Res. Conf. Dig.* **1996**, *54*, 80.
(10) Siegrist, T.; Kloc, C.; Schön, J.; Batlogg, B.; Haddon, R.; Berg, S.; Thomas, G. *Angew. Chem., Int. Ed.* **2001**, *40*, 1732.
(11) Goldmann, C.; Haas, S.; Krellner, C.; Pernstich, K. P.; Gundlach, D. J.; Batlogg, B. *J. Appl. Phys.* **2004**, *96*, 2080.
(12) Kim, E. G.; Coropceanu, V.; Gruhn, N. E.; Sanchez-Carrera, R. S.; Snoeberger, R.; Matzger, A. J.; Brédas, J. L. *J. Am. Chem. Soc.* **2007**, *129*, 13072.
(13) Curtis, M. D.; Cao, J.; Kampf, J. W. *J. Am. Chem. Soc.* **2004**, *126*, 4318.
(14) Brédas, J. L.; Calbert, J. P.; da Silva, D. A.; Cornil, J. *J. Proc. Natl. Acad. Sci. U.S.A.* **2002**, *99*, 5804.
(15) Moon, H.; Zeis, R.; Borkent, E. J.; Besnard, C.; Lovinger, A. J.; Siegrist, T.; Kloc, C.; Bao, Z. N. *J. Am. Chem. Soc.* **2004**, *126*, 15322.
(16) (a) Ando, S.; Murakami, R.; Nishida, J.; Tada, H.; Inoue, Y.; Tokito, S.; Yamashita, Y. *J. Am. Chem. Soc.* **2005**, *127*, 14996. (b) Kojima, T.; Nishida, J.; Tokito, S.; Tada, H.; Yamashita, Y. *Chem. Commun.* **2007**, 1430.
(17) Tan, L.; Zhang, L.; Jiang, X.; Yang, X. D.; Wang, L. J.; Wang, Z.; Li, L. Q.; Hu, W. P.; Shuai, Z. G.; Li, L.; Zhu, D. B. *Adv. Funct. Mater.* **2009**, *19*, 272.
(18) Coropceanu, V.; Cornil, J.; da Silva, D. A.; Olivier, Y.; Silber, R.; Brédas, J. L. *Chem. Rev.* **2007**, *107*, 926.
(19) Xiao, K.; Liu, Y. Q.; Qi, T.; Zhang, W.; Wang, F.; Gao, J. H.; Qiu, W. F.; Ma, Y. Q.; Cui, G. L.; Chen, S. Y.; Zhan, X. W.; Yu, G.; Qin, J. G.; Hu, W. P.; Zhu, D. B. *J. Am. Chem. Soc.* **2005**, *127*, 13281.
(20) Nitzan, A. *Annu. Rev. Phys. Chem.* **2001**, *52*, 681.
(21) Paddon-Row, M. N. *Aust. J. Chem.* **2003**, *56*, 729.
(22) Bixon, M.; Jortner, J. *J. Am. Chem. Soc.* **2001**, *123*, 12556.
(23) Paulson, B. P.; Miller, J. R.; Gan, W. X.; Closs, G. J. *Am. Chem. Soc.* **2005**, *127*, 4860.
(24) Polo, F.; Antonello, S.; Formaggio, F.; Toniolo, C.; Maran, F. *J. Am. Chem. Soc.* **2005**, *127*, 492.
(25) Brédas, J. L.; Deljonne, D.; Coropceanu, V.; Cornil, J. *Chem. Rev.* **2004**, *104*, 4971.
(26) (a) Marcus, R. A. *Rev. Mod. Phys.* **1993**, *65*, 599. (b) Barbara, P. F.; Meyer, T. J.; Ratner, M. A. *J. Phys. Chem.* **1996**, *100*, 13148. (c) Cornil, J.; Brédas, J. L.; Zaumseil, J.; Sirringhaus, H. *Adv. Mater.* **2007**, *19*, 1791.
(27) Fabiano, E.; Della Sala, F.; Cingolani, R.; Weimer, M.; Görling, A. *J. Phys. Chem.* **2005**, *109*, 3078.
(28) Tsai, F. C.; Chang, C. C.; Liu, C. L.; Chen, W. C.; Jenekhe, S. A. *Macromolecules* **2005**, *38*, 1958.
(29) Cao, H.; Ma, J.; Zhang, G.; Jiang, Y. *Macromolecules* **2005**, *38*, 1123.
(30) Hutchison, G. R.; Ratner, M. A.; Marks, T. J. *J. Phys. Chem. B* **2005**, *109*, 3126.
(31) Hutchison, G. R.; Ratner, M. A.; Marks, T. J. *J. Am. Chem. Soc.* **2005**, *127*, 2339.

- (32) Salzner, U.; Lagowski, J. B.; Pickup, P. G.; Poirier, R. A. *Synth. Met.* **1998**, *96*, 177.
- (33) Salzner, U. *Synth. Met.* **2001**, *119*, 215.
- (34) Delley, B. J. *Chem. Phys.* **2000**, *113*, 7756.
- (35) Ye, L.; Freeman, A. J.; Ellis, D. E.; Delley, B. *Phys. Rev. B* **1989**, *40*, 6277.
- (36) Hutchison, G. R.; Zhao, Y.-J.; Delley, B.; Freeman, A. F.; Ratner, M. A.; Marks, T. J. *Phys. Rev. B* **2003**, *68*, No. 035204.
- (37) (a) Zhao, Y.; Truhlar, D. G. *J. Phys. Chem. A* **2004**, *108*, 6908.
- (b) Zhao, Y.; Truhlar, D. G. *J. Chem. Theory Comput.* **2005**, *1*, 415.
- (38) (a) Dkhissi, A.; Blossey, R. *Chem. Phys. Lett.* **2007**, *439*, 35. (b) Gil, A.; Branchadell, V.; Bertran, J.; Oliva, A. *J. Phys. Chem. B* **2007**, *111*, 9372.
- (39) Briseno, A. L.; Miao, Q.; Ling, M. M.; Reese, C.; Meng, H.; Bao, Z. N.; Wudl, F. *J. Am. Chem. Soc.* **2006**, *128*, 15576.
- (40) Frisch, M. J. et al. *Gaussian 03*, Revision D.02; Gaussian Inc.: Pittsburgh, PA, 2006.
- (41) Koopmans, T. *Physica* **1934**, *1*, 104.
- (42) Atkins, P. W. *Physical Chemistry*, 5th ed.; Oxford University Press: Oxford, U.K., 1994.
- (43) (a) Cornil, J.; Lemaire, V.; Calbert, J. P.; Brédas, J. L. *Adv. Mater.* **2002**, *14*, 726. (b) Zhang, Y.; Cai, X.; Bian, Y.; Li, X.; Jiang, J. *J. Phys. Chem. C* **2008**, *112*, 5148. (c) Yang, X.; Wang, L.; Wang, C.; Long, W.; Shuai, Z. *Chem. Mater.* **2008**, *20*, 3205. (d) Song, Y.; Di, C.; Yang, X.; Li, S.; Xu, W.; Liu, Y.; Yang, L.; Shuai, Z.; Zhang, D.; Zhu, D. *J. Am. Chem. Soc.* **2006**, *128*, 15940.
- (44) McCullough, R. D.; Lowe, R. D.; Jayaraman, M.; Anderson, D. L. *J. Org. Chem.* **1993**, *58*, 904.
- (45) Chang, Y. C.; Chen, Y. D.; Chen, C. H.; Wen, Y. S.; Lin, J. T.; Chen, H. Y.; Kuo, M. Y.; Chao, I. *J. Org. Chem.* **2008**, *73*, 4608.
- (46) Lan, Y. K.; Huang, C. I. *J. Phys. Chem. B* **2008**, *112*, 14857.
- (47) (a) Kim, K.; Yoon, Y. K.; Mun, M. O.; Park, S. P.; Kim, S. S.; Im, S.; Kim, J. H. *J. Supercond.* **2002**, *15*, 595. (b) Boronat, M.; Viruela, R.; Orti, E. *Synth. Met.* **1995**, *71*, 2291.
- (48) Rathore, R.; Kochi, J. K. *Adv. Phys. Org. Chem.* **2000**, *35*, 193.
- (49) Kim, W. S.; Kim, J.; Park, J. K.; Mukamel, S.; Rhee, S. K.; Choi, Y. K.; Lee, J. Y. *J. Phys. Chem. B* **2005**, *109*, 2686.